4D Trajectory Optimization Satisfying Waypoint and No-Fly Zone Constraints

4D Trajectory Optimization Satisfying Waypoint and No-Fly Zone Constraints

Daniele Giuseppe Mazzotta, Giuseppe Sirigu
Politecnico di Torino
Department of Mechanical and Aerospace Engineering
Corso Duca degli Abruzzi 24
10129, Torino, ITALY
daniele.mazzotta@polito.it
giuseppe.sirigu@polito.it

Mario Cassaro
ONERA
Dpartement traitement de l'information et systmes
Toulouse, France
Mario.Cassaro@onera.fr

Manuela Battipede, Piero Gili
Politecnico di Torino
Department of Mechanical and Aerospace Engineering
C.so Duca degli Abruzzi 24
10129, Torino, ITALY
manuela.battipede@polito.it
piero.gili@polito.it

Abstract: This paper presents a model of an innovative Flight Management System (FMS) which is purposely developed to control a commercial airliner along an optimized 4-Dimensional Trajectory (4DT), respecting time and path constraints, while avoiding No-Fly Zones (NFZ). The optimum, expressed in terms of minimum fuel consumption, is optained by solving an Optimization Control Problem (OCP) by means of the *Chebyshev Pseudospectral* numerical direct collocation scheme. The OCP trajectory solution is a discrete sequence of optimal aircraft states, which guarantee the *minimum-fuel* trip between two waypoints. With the aim of controlling the aircraft along lateral, vertical and longitudinal axis, and in order to respect NFZ and waypoints constraints along the optimum 4DT, different guidance navigation and control techniques can be implemented. The effectiveness of the algorithms is evaluated through simulations performed in the Multipurpose Aircraft Simulation Laboratory (MASLab), on a Boeing 747-100 model, equipped with a complete Automatic Flight Control System (AFCS) suite.

Key–Words: 4D-Trajectory optimization, no-fly zone, FMS, flight management system, Pseudospectral

1 Introduction

The future revolution of the air traffic system imposes the development of a new class of Flight Management Systems (FMS) [1, 2, 3], capable of providing the aircraft with real-time reference flight parameters, necessary to fly the aircraft through a predefined sequence of waypoints, while minimizing fuel consumption, noise and pollution emissions. The main goal is to guarantee safety operations while reducing the aircraft environmental impact, according to the main international research programs. The requirements that the novel FMS must complies with, are stated in terms of temporal separation defined in a 4D route. The trajectory prediction for the 4DT navigation has a strong impact on the environment, as well as on the operations of the partners involved in the air transport sector. To generate and perform greener trajectories in terms of fuel consumption, emissions and perceived external noise, a trajectory optimization is required.

The 4D trajectory optimization can be addressed by using different techniques. In literature, several papers analyze those techniques and show some application examples. Using direct methods, the trajectory optimal control problem is transformed in a nonlinear programming problem (NLP) where control and state variables time histories, respectively free and constrained variables, are discretized on discretization nodes [4, 5, 6, 7, 8] Approaches not concerning optimal control theory were also proposed in literature to design 4DT [9, 10]. Alam et al. [11] developed a dynamical method to define artificial waypoints to be followed by the aircraft. These waypoints are chosen upon a discretizing grid composed by all possible combinations of nodes in layers defined over the airport area, according to objectives and airplane performance, calculated by using a performance evaluation model like the Base of Aircraft Data (BADA) [12], Piano [13] and the MASLab [14, 13, 15]

On the other hand, once the 4D trajectory is calculated, precise trajectory tracking must be guaranteed by the guidance and control aircraft capabilities. Different guidance and control algorithms for FMSs are proposed in literature for the vertical plane [16, 17, 18, 19] considering also the temporal requirements of the RNP [20]. The Airbus presented an algorithm for the energy management during approach

[21]. Different FMS configurations are presented for both manned and unmanned vehicles [1, 2, 20, 22]. AFCSs and the auto-throttle can be conceived within the FMS itself or external to it; however, low insight is usually given on the AFCS structure and its functions. Conversely, poor attention has been paid in literature to control algorithms able to achieve the novel FMS goals by operating an existing suite of autopilots, with minimum impact on the avionic system architecture. Concerning the lateral plane different solutions are available. Some of these are intended to follow pre-established constant target, whereas others adapt the control of the vehicle to the Air Traffic Management (ATM) contingencies, such as obstacles, air traffic high-density areas, unfavorable weather conditions, etc. In this study, a set of GNC techniques for the FMS of a Boeing 747-100 is presented. With regard to 4DT context, the main purpose of these techniques is to overhaul the Lateral Navigation (LNAV), Time Navigation (TNAV) and Vertical Navigation VNAV of the A/C, to respect the time constraint of the 4DT defined for the last waypoint of a cruise mission. As additional tasks, the FMS is also able to avoid a NFZ, to capture and follow an established route, and finally, to ensure, simultaneously, a minimum fuel consumption trajectory. The NFZ, as well as the cases of re-entry to the established route, can lead to delays in the scheduled time of arrival of the aircraft. The prediction and control of these delays is required in order to avoid an inefficient management of the aircraft performance and airspace. The reasons described above drove the development of new solutions presented in this work. Chapter II presents the numerical method and the A/C model adopted for the solution of the OCP. Chapter III details the guidance navigation and control functions implemented as the kernel of the FMS. Finally, Chapter IV expose the results of the simulations performed by using the Multipurpose Aircraft Simulation Laboratory (MASLab).

2 The Optimal Control Problem

In general terms, the objective of an Optimal Control Problem (OCP) is to determine the control function $u(t) \in \mathbb{R}^m$ and the corresponding state variables $x(t) \in \mathbb{R}^m$ of a given control system, in order to minimize an user-defined cost function J, where $t \in \mathbb{R}$ is the independent time variable, m is the number of controls and n is the number of states.

The purpose of the OCP described in this work is to find the *minimum-fuel* trajectory which leads an A/C to fly a sequence of waypoints, while respecting the Controlled Time of Arrival (CTA), i.e., the time leeway defined by the ATC when the A/C is expected to arrive at the route final waypoint. To this end, the cost function can be expressed as the mass of fuel needed for the flight mission, and it assumes the Bolza form:

$$J(x(t), u(t), t) = \Psi(x(t_0), t_0, x(t_f), t_f) + \int_{t_0}^{t_f} L(x(t), u(t), t)\, dt \quad (1)$$

$\Psi(x(t_0), t_0, x(t_f), t_f)$ is the cost function Mayer term and it depends only on the initial and final value of the state vector, whereas $\int_{t_0}^{t_f} L(x(t), u(t), t)\, dt$ is the Lagrange term which could be evaluated by numerical quadrature1 [23]. For the purpose of this work, Lagrange term was neglected. In order to avoid unfeasible or unrealistic trajectories, the 4DT optimization problem is subject to the A/C dynamic constraints, which in general may be expressed as:

$$\dot{x}(t) = f(x(t), u(t), t), \qquad t \in [t_0, t_f] \quad (2)$$

State and control variables are subjected to the simple bounds:

$$x_l \leq x(t) \leq x_u \quad (3)$$

$$u_l \leq u(t) \leq u_u \quad (4)$$

whereas boundaries conditions are applied by the inequality relation:

$$\psi_l \leq \psi(x(t_0), x(t_f), t_f - t_0) \leq \psi_u \quad (5)$$

The path constraints are introduced in the problem by the inequality:

$$C_l \leq C(x(t), u(t), t) \leq C_u \quad (6)$$

2.1 Pseudospectral Method and Nonlinear Programming Problem

In this section the method used for the OCP solution is presented. Various methods are proposed in calculus of variations literature and all of these are gathered in two main groups: the indirect methods, and the direct methods. Whereas the former aim to solve the necessary conditions derived from the Pontryagin minimum principle [24], the latter achieve a discretization of time history and an approximation of both state and control variables using an accurate interpolation scheme. In this paper, the OCP is solved through a Chebyshev pseudospectral method developed by Ross

and Fahroo [25], and Elnagar and Kazemi [26]. The basic idea behind this direct collocation method is to transform the ordinary differential equations (ODEs) system into an algebraic equations system, by employing jth-degree Lagrange polynomials for the state and control variables. In this manner the state and control variables can be expressed through their values at the Chebyshev-Gauss-Lobatto (CGL) nodes, and the OCP is transformed into a constrained Nonlinear Programming Problem (NLP).The jth-degree Chebyshev polynomial is defined as the unique polynomial satisfying

$$T_j(t) = \cos(j \cdot \arccos(t)) \tag{7}$$

In the Chebyshev pseudospectral method the CGL interpolation nodes are given by

$$t_k = \cos\left(\frac{\pi \cdot k}{N}\right), \qquad k = 0, \ldots, N \tag{8}$$

These nonuniform spaced nodes lies on the interval $[-1, 1]$ and they represent exactly the $N+1$ points where extrema of $T_N(t)$ occour. Since the domain of the Chebyshev polynomial is the interval $[-1, 1]$, a real time history such as $[t_0, t_f]$ needs to be transformed in the interval $[-1, 1]$ by the following linear relation:

$$\begin{gathered}\tau(t) = \left[\frac{(t_f - t_0) \cdot t + (t_f + t_0)}{2}\right] \\ t \in [-1, 1], \tau : [-1, 1] \rightarrow [t_0, t_f]\end{gathered} \tag{9}$$

For sake of readability, the notation will continue to refer to $\tau(t)$. The approximation of state and control vector is addressed by using a linear combination of Lagrange polynomial of the form

$$x^N(t) = \sum_{j=0}^{N} x_j \cdot l_j \tag{10}$$

$$u^N(t) = \sum_{j=0}^{N} u_j \cdot l_j \tag{11}$$

where N is an arbitrary real even or odd, and $N+1$ is the number of CGL points; x_j and u_j are the value of the states and control vectors at the jth CGL nodes and finally, $l_j(t)$ are the Nth-order Lagrangian interpolating polynomial. To obtain an approximation of the derivative $\dot{x}(t)$ at the CGL nodes , Eq. 10 can be differentiated resulting in the following expression:

$$\dot{x}^N(t_k) = \sum_{j_0}^{N} x_j \cdot \dot{l}_j(t_k) = \sum_{j=0}^{N} D_{kj} \cdot x_j, \; k = 0, \ldots, N \tag{12}$$

where D_{kj} are the entries of a $(N+1) \times (N+1)$ differentiation matrix defined in [27]. The matrix D depends only on the number of CGL nodes; thus, once N is fixed, D is a constant matrix. The cost function and state equations are discretized by first substituting Eqs. 10, 11, and 12, in Eqs. 1 and 2, and collocating at the nodes t_k. As a result, the OCP problem is traduced in a NLP: a problem aimed to find the arrays of states $X = (x_0, \ldots, x_N)$ and controls $U = (u_0, \ldots, u_N)$ which minimize the cost function

$$\begin{aligned}J(X, U, t_f) \simeq & \Psi(x_0, t_0, x_N, t_N) + \\ & + \frac{t_f - t_0}{2} \cdot \sum_{k=0}^{N} L(x_k, u_k, t_k) \cdot w_k\end{aligned} \tag{13}$$

subject to

$$\frac{2}{t_f - t_0} \cdot \sum_{j=0}^{N} D_{kj} \cdot x_j = f(x_k, u_k, t_k), \; k = 0, \ldots, N \tag{14}$$

$$\psi_l \leq \psi(x_0, x_N, t_f - t_0) \leq \psi_u \tag{15}$$

$$C_l \leq C(x_k, u_k, t_k) \leq C_u, \qquad k = 0, \ldots, N \tag{16}$$

2.2 The Aircraft Model

The A/C model is represented by a system of mathematical equations which constraint the A/C state and control variables. In parfticular the A/C is modeled by a 3 Degree Of Freedom (3DOF) Aircraft Dynamic Model (ADM), which considers both kinematic and dynamic equations.As the computational effort required by the ADM is significant, it can be substituted by a linear simplified model based on steady state flight conditions which reproduces performance and limitations of the A/C in a steady state condition by using different sets of A/C performance database. The performance steady state data can be extracted from performance calculation tools, such as BADA [12], and the Multipurpose Aircraft Simulation Laboratory (MASLab) [14]. In this study, the steady state performance database is extracted from BADA, whereas MASLab is only used as flight simulator. The state

variables for each CGL node were gathered in a 7-dimension array as

$$x = [N,\ E,\ H,\ m,\ V_{TAS},\ \gamma,\ \psi] \tag{17}$$

where $N,\ E,\ -H$, are the A/C North-East-Down reference frame coordinates, while m is the gross mass of vehicle, V_{TAS} is the A/C true air speed, γ is the flight path angle, and finally ψ is the heading angle. The mathematical model used to describe the A/C dynamic is expressed by

$$\dot{x} = \left\{ \begin{array}{c} \dot{N} = V_{TAS} \cdot \cos\gamma \cdot \cos\psi \\ \dot{E} = V_{TAS} \cdot \cos\gamma \cdot \sin\psi \\ \dot{H} = V_{TAS} \cdot \sin\gamma \\ \dot{m} = -TSFC\left(V_{TAS}\right) \cdot T\left(H\right) \\ \dot{V}_{TAS} = \frac{1}{m} \cdot (T - D - m \cdot g \cdot \sin\gamma) \\ \dot{\gamma} = \frac{1}{m \cdot V_{TAS}} \cdot (L \cdot \cos\phi - m \cdot g \cdot \cos\gamma) \\ \dot{\psi} = \frac{L \cdot \sin\phi}{m \cdot V_{TAS} \cdot \cos\gamma} \end{array} \right\} \tag{18}$$

where the first three equations represent only the kinematic constraints, $\dot{m}$ is the BADA fuel flow prediction for the cruise phase, ϕ is the roll angle, and the last three equations are the dynamic constraints more representative for the flight mission considered in this study.

2.3 The Path Constraints

Cruise endpoints, traffic separation aspects, terrain obstacles, weather hazards, noise sensitive areas, and persistent contrail formation region, are all examples of path constraints that can be included in the trajectory optimization problem. In addition to this, the flight plan constraints can be added to the 4DT optimization problem as speed, altitude or time constraints. With the exception of the cruise endpoints and flight plan constraints, the previous path constraints were represented by a No-Fly Zone (NFZ), namely an airspace region or volume with definite boundaries where the flight is restricted or permanently forbidden.

3 Guidance Navigation and Control Techniques for 4DT

In this section, the set of Guidance Navigation and Control (GNC) techniques for the novel FMS are presented. The main scope of these techniques is to achieve all the functions required for the 4DT navigation:

1. Navigation function, including measurement of A/C states and prediction of the optimized trajectory;
2. FMS and Automatic Flight Control System (AFCS) target generation;
3. Guidance and control functions for the Vertical Navigation (VNAV), Lateral Navigation (LNAV), and Time Navigation (TNAV).

The navigation function is common to all control axes (vertical, lateral and longitudinal axes). The target generation function, instead, needs to focus on which type of control is used for each AFCS axis. In general, the AFCS targets are: the bank angle ϕ_d, the pitch angle θ_d, the Throttle Lever Angle (TLA) Π, the Indicate Air Speed (IAS) target V_{IAS}, and finally, the altitude target H_d. These are the targets provided by GNC algorithms to the AFCS to address the VNAV, the LNAV and the TNAV of a generic 4DT. The schematic of the FMS functions and AFCS-A/C interface are depicted in Figure 1.

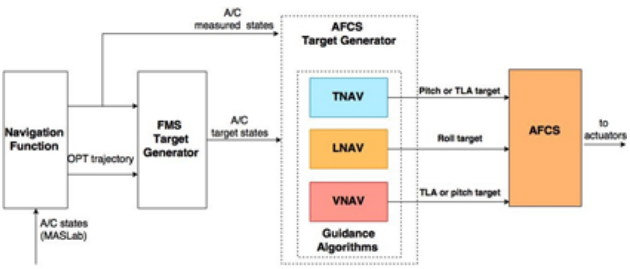

Figure 1: Scheme of the Flight Management System and its context.

3.1 The Navigation Function and FMS Targets

The assumption to use the states generated by the A/C simulator as measured states strongly simplifies the navigation function. In this approach, the navigation function was essentially reduced in: a mere junction for the A/C states, a navigation database containing the optimized trajectory, and finally in an algorithm to compute the distance flown along the established route i.e., an Along Path Distance (APD) calculator. As far as the last point is concerned, the addition of the time variable to the classical 3D route leads to know, at each time, the APD flown by the A/C along the established route. Indeed, since the OCP solution is a set of time-based A/C states, the FMS has to be able to compute the discrepancy between where the A/C is expected to be at the current time, and where the A/C effectively is at the cur-

rent time. In other words, in order to generate targets that are based on the position of the A/C with respect to the established route, the *time-based* OCP trajectory (e.g., $N(t), E(t), H(t), V_{TAS}(t)$, etc.) has to be transformed in a *position-based* trajectory (e.g., $N(R(t)), E(R(t)), H(R(t)), V_{TAS}(R(t))$). The task of calculating the APD $R(t)$ is addressed by a specific algorithm called APD calculator, whereas the function of expressing the optimum targets $X_{opt}(R(t))$ as a function of the APD flown, is achieved by a series of look-up tables in the FMS targets generation function.

3.2 The AFCS Targets

In general, an AFCS is meant to provide the air vehicle control surfaces actuators with the necessary commands to fly the A/C toward a specified attitude target. This objective is addressed by activating different control logics, called also modes, which operate on three distinct A/C control axes: vertical axis (pitch modes), lateral axis (roll modes), and longitudinal axis (autothrottle modes). Table 1 gathers all the MASLab [15] AFCS modes available for each axis of control. At any time, only one single mode can be active for each axis.

The terms manual and managed depend on whether AFCS is controlled by the pilot or by FMS respectively. For the purpose of this study, only the managed modes were used. In particular, for the pitch axis, VNAV PATH, VNAV SPD or VNAV ALT aims to maintain a desired pitch angle θ_d, an IAS V_{IAS}, or an altitude target H_d respectively. For the lateral axis, only one managed mode exists and it is aimed to maintain a desired roll angle ϕ_d. Finally, three managed modes are available for the longitudinal axis: THR REF, SPD, and MACH .They can be used to maintain a desired TLA Π_d, an IAS V_{IAS}, or a Mach target M respectively. Since the implementation of the GNC techniques required in 4DT guidance has to work along the same lines of the design of AFCS modes, it was of paramount importance to understand the MASLab AFCS functionalities. For more details concerning how the MASLab AFCS modes work, refer to [15].

3.3 The Vertical Navigation

The purpose of the Vertical Navigation (VNAV) is to control the A/C attitude along the vertical axis. Therefore, VNAV has to generate the AFCS targets required to follow a specified vertical profile expressed in terms of altitude target H_d. The AFCS has two targets that can be used for this purpose: the pitch angle θ and throttle Π. The algorithm used to generate this commands are two, and both use a Proportional-Derivative (PD) controller to contain the altitude error between the OCP target altitude H_d, and the current altitude H of the A/C. When the elevator is chosen to control the altitude, the PD controller generates the pitch angle target θ_d as:

$$\Delta H = H_d(R(t)) - H \tag{19}$$

$$\Delta\theta = \theta_d - \theta = K_P \cdot \Delta H + K_d \cdot \frac{dH}{dt} \tag{20}$$

where indicates the altitude error (the difference between the desired altitude H_d and the A/C current altitude H), and K_p and K_d are, respectively, the proportional and derivative gains of the PD controller. The pitch target θ_d is then sent to the VNAV PATH mode of the MASLab AFCS, which is the responsible to send to the actuators the commands needed to follow the desired altitude target.

When the throttle is used to control the altitude of the A/C, the PD controller generates the target Π_d as a function of altitude error similarly to Eq. 20, and Π_d is then sent to the Managed THR REF mode of the AFCS.

3.4 The Lateral Navigation

The projection of the optimum trajectory of the A/C on the North-East plane, is a sequence of route legs leading from the first waypoint to the last waypoint of the cruise flight plan. In order to track an established route on the lateral-directional plane of the A/C, the FMS should be able to break the directional path into a sequence of basic lateral maneuvers. The Lateral Guidance Manager (LGM) is the main algorithm that addresses this task, and it can be considered as the kernel of the lateral control along the established route. The LGM developed in this work is based on the work did by Peters and Konyak [28].

Once the A/C initial position is well established by Navaids, and route data uploaded in the FMS by the optimization process, the LGM knows all the maneuvers that form the flight plan and it generates the required targets for the LNAV. *Route Following* and *Route Capture* are the principal sets of maneuvers used to control the A/C along lateral axis. By using a combination of these, the A/C can starts from any initial condition and fly until the end of the route. Figure 2 illustrates a generic flight mission conducted by the LGM guidance.

For the sake of conciseness, only the control law used during the Route Following is explained here. During this maneuver, the A/C has to maintain the

Table 1: Manual and managed modes of the MASLab Automatic Flight Control System.

Mode type	**Pitch**	**Roll**	**Autothrottle**
Manual	MAN ALT VS IAS GS TOGA	MAN HDG TRK LOC TOGA	THR HOLD THR REF SPD MACH
Managed	VNAV PATH VNAV SPD VNAV ALT	LNAV	Managed THR REF Managed SPD Managed MACH

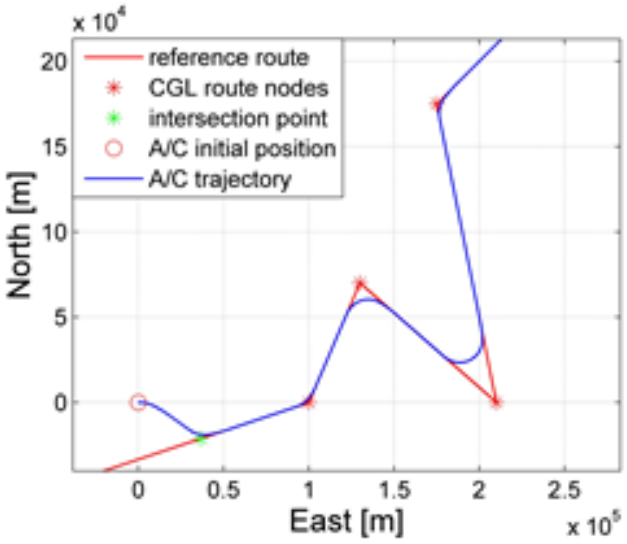

Figure 2: Example of a generic flight mission conducted by the LGM guidance.

desired segment course (heading angle) and eliminate the lateral separation from the established route. The lateral separation, here indicated as Cross Track Error (CTE), is processed by a Proportional-Integrative-Derivative (PID) controller, which provides a desired target for the bank angle. The commands provided by the PID, summed to the signals originated by the HDG mode of the AFCS, produce a desired bank angle based on the magnetic course and on the lateral separation from the route. The control law is mathematically described by the following equation:

$$\begin{aligned}\Delta\phi =&\phi_d - \phi = K_p \cdot \Delta\psi + \\ &+ K_{pCTE} \cdot CTE + K_{dCTE} \cdot \frac{dCTE}{dt} + \\ &+ K_{iCTE} \cdot \int CTE \cdot dt\end{aligned} \tag{21}$$

where $\Delta\psi$ indicates the error between the desired heading angle ψ_d and the current A/Cs heading angle ψ, K_p is the proportional gain that needs to be scheduled with A/C TAS, whereas $K_{pCTE}, K_{dCTE}, K_{iCTE}$ are, respectively, the proportional, derivative and integrative gains of the PDI controller.

Triggering the target generation for the other control axes is an important aspect of the LNAV. Indeed, in order to generate targets that are position-based, the LNAV should provide the other axis with the information about the relative location of the A/C with respect to the established route. The Route Following guidance for the LNAV represents the best instrument to communicate to other axis which route segment the A/C is currently flying. Figure 3 shows the flow chart implemented in the state machine for the Route Following guidance. The control logic governs the activation of the track-to-fix maneuver and the fly-by maneuver iteratively. When the transition maneuver ends (i.e. when A/C it is aligned with the next route segment), the state machine generates the shift signals that advises the passage from the current route leg to the subsequent one.

3.5 The Time Navigation

In order to completely define a 4DT, each waypoint forming the route must be associated with an Established Time of Arrival (ETA). In this research, the ETA are the CGL time nodes of the OCP solution. The Controlled Time of Arrival (CTA), instead, is the

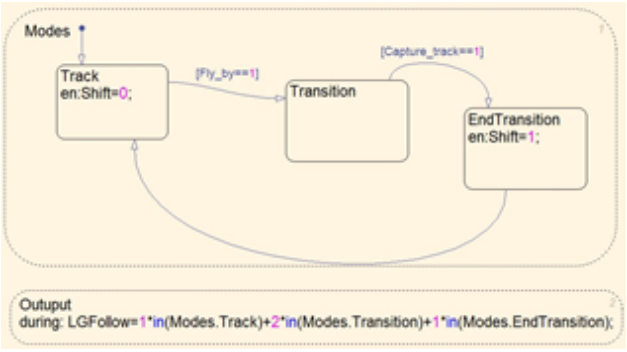

Figure 3: Flow chart of the Route Following guidance.

time constraint defined for the initial and last waypoint of the cruise phase. When a CTA is set for the last waypoint of the established path (CTA of the first waypoint is set to simulation time zero), the goal of TNAV is to provide the A/C speed changes needed to contain errors between the CTA and the effective Time Of Arrival (TOA) at the last waypoint. Therefore, the FMS has to generate an airspeed target profile for the AFCS, as well as the control signals required for the longitudinal axis (i.e., pitch angle or the TLA), to respect the time constraints at each waypoint.

The TNAV control law used in this study is a slight modification of the Interval Management (IM) algorithm developed by Bai, Vaddi, and Mulfinger [29]. As a general concept, the IM strategy is aimed to maintain a longitudinal separation between two vehicles (Target A/C and Ownship A/C) during the approach, when they are equipped with ADS-B (Automatic Dependent Surveillance-Broadcast) system. Since no Target vehicle was considered in this work, the longitudinal separation was to set to be equal to the CTA of the last waypoint. As a result of these assumptions, the error in TOA of the Ownship A/C simply is:

$$e_{TOA} = t - t_{opt}\left(R\left(t\right)\right) \tag{22}$$

where t is the current simulation time and $t_{opt}\left(R\left(t\right)\right)$ is the expected time of arrival based on the reference trajectory (ETA). The time error sign is positive when A/C is delayed and negative when the A/C is anticipating the established route. The speed variation used to reduce the TOA error follows a proportional law of the form

$$\Delta V = k_v \cdot e_T OA \tag{23}$$

where the gain k_v has the dimension of an acceleration, and it dictates how much speed variation is commanded per each second of error. The A/C TAS target V_{com} is defined as

$$V_{com} = V_{TAS} + \Delta V, \quad \Delta V \in [0, 0.1 \cdot V_{TAS}] \tag{24}$$

Moreover, in order to prevent strong variations in airspeed target value, the incremental speed command was bounded to be less than 10% of current A/C TAS.

The IM algorithm used to generate the TNAV targets is therefore represented by the Eqs. 23 and 24. However, the speed target admitted by AFCS is expressed as IAS, so a previous conversion from TAS to IAS is needed. The algorithm described until here is the target generator for the TNAV axis. The control laws used to capture and maintain the speed target values were chosen among the AFCS modes of MASLab. Two control targets can be chosen: the pitch angle θ or the TLA Π. Hence, when the control along longitudinal axis is carry out by the elevator command, the VNAV SPD mode is used; conversely, when speed control is addressed by using the throttle command, the A/T SPD mode is used.

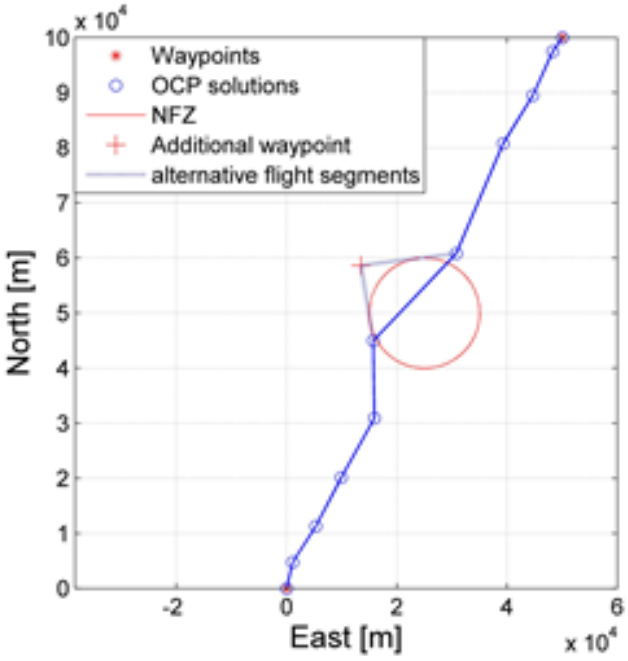

Figure 4: Example of optimum trajectory crossing the NFZ.

Another interesting task addressed by the TNAV is related to the presence of the NFZ. The optimal cruise trajectory is a discrete sequence of A/C states calculated at the CGL time grid. Thus, the derived reference trajectory is approximated by a piecewise linear curve, which links the CGL nodes in the North-East plane of the A/C. Although the discrete solutions singularly falls outside the NFZ, the flight path between two nodes may cross the NFZ. In order to avoid the NFZ during the flight, an additional waypoint is

needed. The additional waypoint is positioned at the intersection of two segments tangent to the NFZ. This situation is represented in Figure 4. Since the additional waypoint is not part of the OCP solution, the optimal states in that point have to be extrapolated. Whereas the mass and altitude values were interpolated linearly, the generation of the TAS target is governed by the *spread* algorithm. The strategy is to produce different TAS profiles, depending on the number of waypoints after which the A/C want to recover the delays due to the NFZ detour. If n_{split} is the number of waypoints (after the additional one) after which the A/C would have to respect the optimum time constraint $t_{opt}\left(R\left(t\right)\right)$, $\bar{V}_{TAS}$ is the constant speed that has to be maintained to recover the delay due to the detour. $\bar{V}_{TAS}$ target for n_{split} nodes is obtained by using the simple cinematic relation

$$\bar{V}_{TAS} = \sum_{k=1}^{n_{split}+1} ldev_k / \left(t_{n+n_{split}} - t_n\right) \qquad (25)$$

where $ldev_k$ is the length of the kth-leg considered in NFZ detouring, and is the CGL node in which deviation should start.

4 Results

The results of the optimal cruise simulation are presented in this section. The mission was to guide an A/C from the initial waypoint WP_i until the terminal waypoint WP_f of the cruise phase, satisfying the time constraint, minimizing the fuel consumption, and avoiding a NFZ placed along the cruise path. The Above Ground level (AGL) of the cruise endpoints was set to 10887 m. The NFZ was envisaged as a cylinder of radius 10 km with no lower and upper bounds and centered in the point of coordinates [100km North, 100Km East], so that its projection on the North-East plane is a 2D circular area. The CTA at WP_f was set to 2000 s, and it was calculated as the time needed to fly from the first waypoint to the last waypoint of in straight line, maintaining a cruise TAS of $242\,m/s$. The different GNC algorithms were combined in order to accurately observe the A/C behavior when TNAV, LNAV, and VNAV are operating simultaneously. For each axis of control, a target generator and an AFCS mode (as interpreter of the targets) has to be assigned:

- VNAV - AFCS mode: VNAV ALT (θ_d); target generator: none, the target is directly H_d;
- LNAV - AFCS mode: LNAV (ϕ_d); target generator: Lateral Guidance Manager (LGM);
- TNAV - AFCS mode: A/T SPD (Π_d); target generator: Interval Management (IM);

Table 2 contains the data which define the optimum reference 4DT. The symbol + refers to the additional waypoint and ETA are calculated for n_{split} equal to one. Figure 5 represents the projection of the A/C trajectory on the North-East plane when FMS 1 is adopted in the simulation.

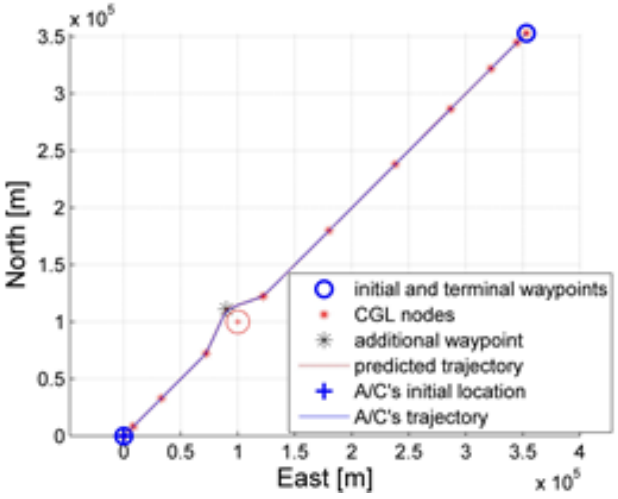

Figure 5: Projection of the A/C trajectory on the North-East plane.

Table 3 collects the relative errors in TOA. If RNAV 2 is imposed longitudinally [30, 31] on the last waypoint, the A/C exceeds the longitudinal limit only during 10.05 s. When comparing this interval with the total duration of the simulation (2000 s), the flight is in compliance with the RNAV requirements. Figures 6 and 7 show the target profiles followed by the FMS for two cases. The trend of V_{TAS} target depends on how many waypoint are chosen to spread the NFZ avoidance in space and in time. When n_{split} is one (Figure 7), the LNAV accelerates the A/C to recover the reference TOA on the first waypoint after the NFZ. The sharp peak in correspondence of the additional waypoint could lead the A/C beyond the envelope limits. To solve this problem, and create a smoother speed profile, n_{split} was set to be equal to three (Figure 6).

Figure 8 shows the trend of the A/C gross weight during the simulation. There is a strong divergence between the A/Cs gross mass established by MASLab simulator (blue line), and the mass value established by the OCP (red dotted line). The total fuel consumption predicted by the OCP was $6284.8\,kg$, whereas the fuel burned estimated by MASLab during the cruise mission was $7442\,kg$. The error ($1157.1\,kg$) represents almost 16% of the total fuel burned. The cause of this error stems from two reasons: the presence of

Table 2: Optimum reference trajectory at the CGL.

CGL	1	2	3	4	+	5	6	7	8	9	10	11
North [km]	0	8.4	33	72.16	111	122.52	180	238.13	286.56	321.93	344.65	353
East [km]	0	8.4	33	72.16	90	122.49	180	238.13	286.58	321.94	344.66	353
AGL[km]	10.89	10.89	10.89	10.89	10.92	10.95	10.89	11.27	11.73	11.61	11.22	10.89
ETA [s]	0	49	191	412	566	691	1000	1309	1588	1809	1951	2000

Table 3: Time results.

CGL	1	2	3	4	+	5	6	7	8	9	10	11
ETA [s]	0	49	191	412	566	691	1000	1309	1588	1809	1951	2000
TOA [s]	0	49	191	412	574	699	1003	1312	1588	1807	1950	2000
e_{TOA} [s]	0	0.2	0.2	0.3	7.2	8	3.2	2	0	-2.3	-1.1	0.2

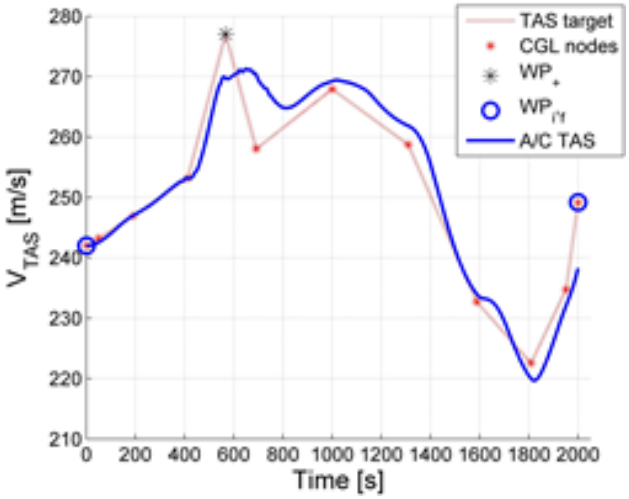

Figure 6: TAS target and A/C TAS profile adopting $n_{split} = 1$.

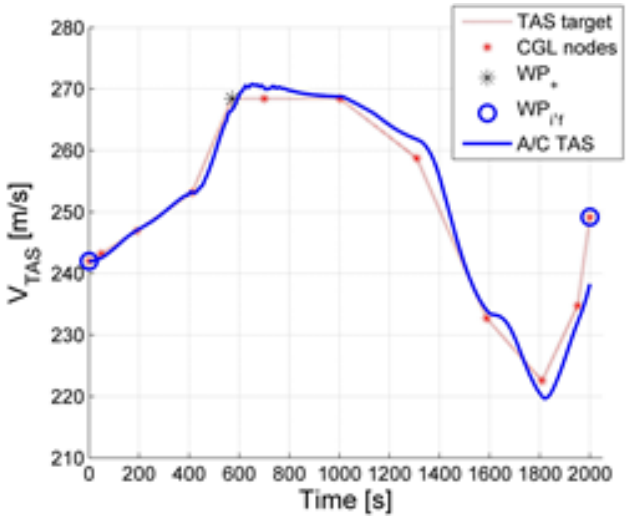

Figure 7: TAS target and A/C TAS profile adopting $n_{split} = 3$.

a NFZ, and the discrepancies between the OCP fuel consumption model (BADA) and the model embedded in MASLab. As far as the first reason is concerned, the deviation due to the NFZ, as well as the speed changes aimed to respect the time constraint over the NFZ, are all aspects not considered by the optimization process. Further, both BADA and MASLab models are not perfect, so they cannot perfectly predict the fuel consumption at each instant of cruise mission.

5 Conclusion

The results of MASLab simulations show, in the first place, a satisfactory aptitude of the innovative LNAV and TNAV control techniques to perform a 4DT navigation. In particular, the results show that LNAV is the best solution to communicate to the other control axis the transition between the different route legs. Secondly, the results demonstrat a strong adherence with time windows defined for the 4DT along the longitudinal axis. The work done is not exhaustive for the flight simulation context, as well as for the field of tra-

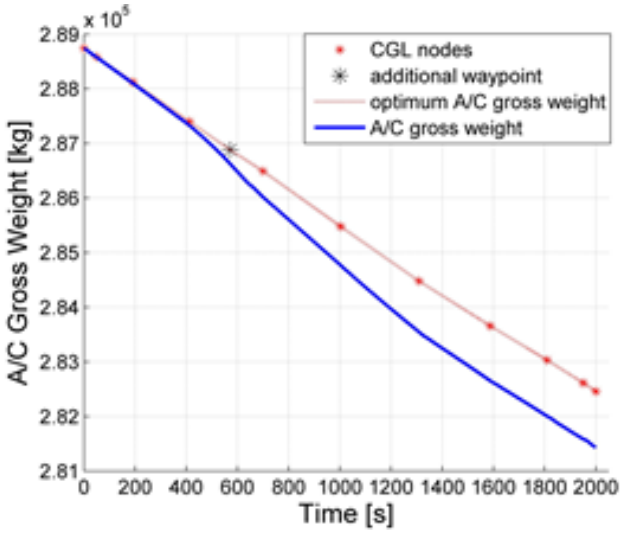

Figure 8: A/C gross mass adopting $n_{split} = 3$.

jectory optimization. The LNAV could be enhanced by defining new lateral maneuvers e.g., fly-over waypoints and holding patterns. Further works are needed to address route optimization processes able to consider dynamic 3D NFZ, multi A/C scenarios, as well as real atmosphere and wind model scenarios.

References:

[1] S. Ramasamy, R. Sabatini, A. G. Gardi, and Y. Liu, "Novel flight management system for real-time 4-dimensional trajectory based operations," in *AIAA Guidance, Navigation, and Control (GNC) Conference*, p. 4763, 2013.

[2] S. Ramasamy, R. Sabatini, A. Gardi, and T. Kistan, "Next generation flight management system for real-time trajectory based operations," *Applied Mechanics and Materials*, vol. 629, pp. 344–349, 2014.

[3] G. Sirigu, M. Battipede, P. Gili, and M. Cassaro, "FMS and AFCS interface for 4D trajectory operations," tech. rep., SAE Technical Paper, 2015.

[4] J. T. Betts, "Survey of numerical methods for trajectory optimization," *Journal of guidance, control, and dynamics*, vol. 21, no. 2, pp. 193–207, 1998.

[5] J. Betts and I. Kolmanovsky, "Practical methods for optimal control using nonlinear programming," *Applied Mechanics Reviews*, vol. 55, p. B68, 2002.

[6] J. Vlassenbroeck, "A chebyshev polynomial method for optimal control with state constraints," *Automatica*, vol. 24, no. 4, pp. 499–506, 1988.

[7] J. Vlassenbroeck and R. Van Dooren, "A chebyshev technique for solving nonlinear optimal control problems," *IEEE transactions on automatic control*, vol. 33, no. 4, pp. 333–340, 1988.

[8] M. Battipede, G. Sirigu, M. Cassaro, and P. Gili, "Analysis of the impact of performance model accuracy on 4d trajectory optimization," in *AIAA Modeling and Simulation Technologies Conference*, p. 0145, 2015.

[9] A. Olivares, M. Soler, and E. Staffetti, "Multiphase mixed-integer optimal control applied to 4d trajectory planning in air traffic management," in *Proceedings of the 3rd International Conference on Application and Theory of Automation in Command and Control Systems*, pp. 85–94, ACM, 2013.

[10] Y. Matsuno, "Stochastic conflict-free 4d trajectory optimization in the presence of uncertainty," in *Proceedings of the 29th Congress of the International Council of Aeronautical Sciences*, pp. 1–21, 2014.

[11] S. Alam, M. Nguyen, H. Abbass, C. Lokan, M. Ellejmi, and S. Kirby, "A dynamic continuous descent approach methodology for low noise and emission," in *Digital Avionics Systems Conference (DASC), 2010 IEEE/AIAA 29th*, pp. 1–E, IEEE, 2010.

[12] A. Nuic, "User manual for the base of aircraft data (BADA) revision 3.10," *Atmosphere*, vol. 2010, p. 001, 2010.

[13] L. Ltd, "Piano aero."

[14] M. Cassaro, P. Gunetti, M. Battipede, and P. Gili, "Overview of the multipurpose aircraft simulation laboratory experience," in *2013 Aviation Technology, Integration, and Operations Conference*, p. 4306, 2013.

[15] P. Gunetti, M. Cassaro, M. Battipede, and P. Gili, "Modeling autopilot suites for a multi-aircraft simulator," in *AIAA Modeling and Simulation Technologies (MST) Conference*, p. 4736, 2013.

[16] H. Bouadi and F. Mora-Camino, "Space-based nonlinear dynamic inversion control for aircraft continuous descent approach," in *Evolving and Adaptive Intelligent Systems (EAIS), 2012 IEEE Conference on*, pp. 164–169, IEEE, 2012.

[17] H. Bouadi and F. Mora-Camino, "Aircraft trajectory tracking by nonlinear spatial inversion," in *AIAA Guidance, Navigation, and Control Conference*, p. 4613, 2012.

[18] B. L. Stevens, F. L. Lewis, and E. N. Johnson, *Aircraft control and simulation: dynamics, controls design, and autonomous systems*. John Wiley & Sons, 2015.

[19] L. Stell, "Flight management system prediction and execution of idle-thrust descents," in *Digital Avionics Systems Conference, 2009. DASC'09. IEEE/AIAA 28th*, pp. 1–C, IEEE, 2009.

[20] M. G. Ballin, D. H. Williams, B. D. Allen, and M. T. Palmer, "Prototype flight management capabilities to explore temporal rnp concepts," in *Digital Avionics Systems Conference, 2008. DASC 2008. IEEE/AIAA 27th*, pp. 3–A, IEEE, 2008.

[21] *Flight Operations Brieng Notes - Approach Techniques Aircraft Energy Management during Approach*. Airbus S.A.S., October2015.

[22] A. F. Tarhan, E. Koyuncu, M. Hasanzade, U. Ozdemir, and G. Inalhan, "Formal intent based flight management system design for unmanned aerial vehicles," in *Unmanned Aircraft Systems (ICUAS), 2014 International Conference on*, pp. 984–992, IEEE, 2014.

[23] C. W. Clenshaw and A. R. Curtis, "A method for numerical integration on an automatic computer," *Numerische Mathematik*, vol. 2, no. 1, pp. 197–205, 1960.

[24] L. S. Pontryagin, *Mathematical theory of optimal processes*. CRC Press, 1987.

[25] F. Fahroo and I. M. Ross, "Direct trajectory optimization by a chebyshev pseudospectral method," *Journal of Guidance, Control, and Dynamics*, vol. 25, no. 1, pp. 160–166, 2002.

[26] G. N. Elnagar and M. A. Kazemi, "Pseudospectral chebyshev optimal control of constrained nonlinear dynamical systems," *Computational Optimization and Applications*, vol. 11, no. 2, pp. 195–217, 1998.

[27] L. N. Trefethen, *Spectral methods in MATLAB*. SIAM, 2000.

[28] M. Peters and M. A. Konyak, "The engineering analysis and design of the aircraft dynamics model for the faa target generation facility," *Seagull Technology, Inc., Los Gatos, CA*, pp. 43–45, 2003.

[29] X. Bai, S. Vaddi, and D. G. Mulfinger, "Evaluation of temporal spacing errors associated with interval management algorithms," in *14th AIAA Aviation Technology, Integration, and Operations Conference*, p. 3154, 2014.

[30] I. Doc, "Procedures for air navigation services–aircraft operations–volume ii–construction of visual and instrument flight procedures," *International Civil Aviation Organisation,*, vol. 5, 2006.

[31] I. Doc, "Performance based navigation (pbn) manual," *Montréal: International Civil Aviation Organisation*, 2008.